University of Nebraska - Lincoln

DigitalCommons@University of Nebraska - Lincoln

Architectural Engineering -- Faculty Publications

Architectural Engineering

2017

Study on the methods for predicting the performance of a hybrid solar-assisted ground-source heat pump system

Zhaoyi Zhuang
University of Nebraska - Lincoln, hit6421@126.com

Qiqi Zhu
Shandong Jianzhu University

Jian Song
Shandong Jianzhu University

Xin Zhang
Shandong University

Haorong Li
University of Nebraska-Lincoln, hli3@unl.edu

Follow this and additional works at: https://digitalcommons.unl.edu/archengfacpub

Part of the Architectural Engineering Commons, Construction Engineering Commons, Environmental Design Commons, and the Other Engineering Commons

10th International Symposium on Heating, Ventilation and Air Conditioning, ISHVAC2017, 19-22 October 2017, Jinan, China

Study on the methods for predicting the performance of a hybrid solar-assisted ground-source heat pump system

Zhaoyi Zhuang[a,b,c,] [*], Qiqi Zhu[a], Jian Song[a], Xin Zhang[d], Haorong Li[b]

[a]School of Thermal Engineering, Shandong Jianzhu University, Jinan 250101, China
[b] Durham School of Architectural Engineering & Construction, University of Nebraska–Lincoln, Omaha68182, USA,
[c]Shandong Zhongrui New Energy Technology Co., Ltd. Jinan250101, China
[d] School of Information Science and Engineering, Shandong University, Jinan 250100, China

Abstract

It is critical to find suitable setting parameters for designing a hybrid solar-assisted ground-source heat pump system in the practical engineering application, but the heat pump performance is unpredictable after many years of operation. This paper used 2000 sets of performance data collected from solar-assisted GSHP systems that keep operating over 20 years to simulate long term used heat pump with a professional software called GeoStar. Adopted the classification and regression tree (CART) method, the design of solar energy collector areas can be predicted. The multi-linear regression is also utilized to predict average monthly per meter borehole heat exchange. Seasonal factor decomposition and exponential smoothing are used to analyze the average monthly temperature of the circulating fluid, circulating fluid inlet and outlet temperatures of the heat pump after 20 years when we perform the time series prediction. Experimental results demonstrate that CART, multi-linear regression, seasonal factor decomposition and exponential smoothing are promising for practical applications.

© 2017 The Authors. Published by Elsevier Ltd.
Peer-review under responsibility of the scientific committee of the 10th International Symposium on Heating, Ventilation and Air Conditioning.

*Keywords:*a hybrid solar-assisted ground-source heat pump system; GeoStar software; prediction methods;

1. Introduction

Nowadays, the environmental and natural resources have become key factors in the sustainable development of a country. It is challenging to balance the resource consumption (such as mineral resources) with clean environment.

*Corresponding author. Tel:+86 18906442878
*E-mail address:*hit6421@126.com

A vision to solve this challenge is to employ green, pollution-free alternative energy source. This paper approaches this vision by a ground-source heat pump (GSHP) [1]. The GSHP system performance degrades if installed in heating-dominated buildings in severe cold climate areas, where more heat are extracted from the ground than rejected into the ground. This will cause a lower temperature in the intake water due to the annual released heat. A solution is to increase the spacing between boreholes, or to use strip type and block layout with a high level of initial investment to eliminate this thermal imbalance[2]. Chen and Yang designed and numerically simulated a solar assisted GCHP system in northern China[3], which showed that this optimal design reduced the borehole length of 3.9m/m² and the designed system efficiency could be 3.55 with 36% annual space heating solar fraction and 75% annual domestic hot water solar fraction. Verma et al [4] studied the solar energy storage and space heating by using solar-assisted GCHP system for Indian climatic conditions. Man and Yang [5] simulated hybrid GSHP system with heat transfer process of principal components model, and combined nocturnal cooling radiator works with hybrid GSHP system[6]. Youet al [7] proposed multiple functions, such as heat compensation, direct domestic hot water (DHW) as well as direct space heating, to support heat compensation unit with thermosyphon unit for the purpose of energy-saving of hybrid GCHP system in cold regions requiring considerable air-conditioning and DHW supply[8]. In our previous work [9], we have used Partial Least Squares Regression (PLSR), Support Vector Regression (SVR) and M5 Model Tree to predict the heat transfer performance for the GCHP system. However, there has been little work on predicting the performance of solar-assisted ground-source heat pump systems. To address the problem, 2000 groups of simulation data of solar-assisted GSHP systems operating for over 20 years were created using simulation with a professional software GeoStar [10]. Then, the classification and regression tree (CART), multi-linear regression, and time series analysis are used to predict the performance of solar-assisted ground-coupled heat pump system.

2. Data collation analysis

This paper employs 2000 sets of performance data simulated from a professional software called GeoStar[10]. Collector area Y_1, average monthly per meter borehole heat exchange Y_2, average monthly temperature of the circulating fluid Y_3, circulating fluid inlet temperature of the heat pump Y_4 and circulating fluid outlet temperature of the heat pump Y_5. Y_2, Y_3, Y_4 and Y_5 are all time series data for 240 months (20 years). The system working condition parameters includes drilling vertical spacing X_1, drilling column spacing X_2, drilling radius X_3, drilling geometry arrangement X_4, drilling nominal external diameter X_5, U-tube spacing X_6, thermal conductivity coefficient X_7, drilling depth X_8, number of drilling X_9, ground temperature X_{10}, ground thermal conductivity X_{11}, circulating fluid parameter X_{12}, collector type X_{13}, collector efficiency X_{14}, collector installation angle X_{15}, heat loss efficiency X_{16} and surface albedo X_{17}. X_4, X_6 X_{11} and X_{12} are catalog, and their introduction can be found in Ref [9]. X_{13} Is also catalog, and Table 1 provides the specific collector type X_{11} of different materials in this study. Table 2 provides descriptive statistics of these 17 system working condition parameters.

Table 1. Collector type X11

Nominal value	Meaning
1	metallic glass vacuum tube
2	flat-plate collector
3	glass tube collector with vacuum

Table 2. Statistics of these 17 pump working condition parameters

Parameters	X_1	X_2	X_3	X_4	X_5	X_6	X_7	X_8	X_9
Average	3.998	4.000	0.065	2.88	36.75	2.50	2.034	96.16	59.07
Standard deviation	0.708	0.707	0.007	1.453	9.313	1.118	0.455	13.317	8.210
Minimum	2.5	3	0.055	1	25	1	1.3	80	46
Maximum	5	5	0.075	5	50	4	2.8	120	70
Range	2.5	2	0.02	4	25	3	1.5	40	24

Parameters	X_{10}	X_{11}	X_{12}	X_{13}	X_{14} / %	X_{15}	X_{16} / %	X_{17}
Average	15.00	4.47	5.84	2.00	59.98	42.39	14.33	0.168
Standard deviation	3.161	2.283	3.234	0.817	7.076	8.575	7.085	0.058
Minimum	10	1	1	1	50	30	5	0.10
Maximum	20	8	11	3	70	55	25	0.25
Range	10	7	10	2	20	25	20	0.15

3. Simulation and calculation

3.1 Performance Prediction on Y_1

Generally speaking, when establishing and training the prediction model, addition of unnecessary features will reduce the prediction performance. Moreover, a wide difference between the value ranges of different features will also affect the regression prediction. Therefore, we mainly adopt feature selection and normalization to preprocess the original data.

3.1.1 Feature Selection

Feature selection is a procedure that investigates all the features to eliminate irrelevant ones, and the standards for investigation vary. Now, data used in this paper are mainly studied in two aspects: variance and correlation.

Variance：

$$S^2 = \frac{1}{N} \sum_{i=1}^{n} \left(x_i - \overline{x} \right)^2 \tag{1}$$

where $\overline{x}$ is mean of a set $\{x_i, i = 1, \cdots, N\}$, and N is the size of the set.

Pearson correlation coefficient：

$$r = \frac{1}{N-1} \sum_{i=1}^{n} \left(\frac{x_i - \overline{x}}{S_x} \right) \left(\frac{y_i - \overline{y}}{S_y} \right) \tag{2}$$

where S_X and S_Y are standard deviations of $\{x_i, i = 1, \cdots, N\}$ and $\{y_i, i = 1, \cdots, N\}$, and $\overline{y}$ is mean of a set $\{y_i, i = 1, \cdots, N\}$. Pearson Correlation Coefficient ranging in value from -1 through +1, +1 means that there is a positive linear correlation between two variables, -1 means that there is a linear negative correlation, and 0 means irrelevance.

Firstly, the variances of 17 variables are calculated and the threshold, as shown in Fig.1, was set to 0.1. Meanwhile, any feature whose variance is lower than 0.1 among the 2000 samples will be eliminated for it cannot show sufficient differences and has a little help in establishing the model. Feature X_3 and X_{17} are eliminated during the regression prediction of Y_1 for smaller variances.

Single variable selection then is processed after eliminating features with variance lower than the threshold, where Pearson correlation coefficient is used in the measurement of correlation. Consequently, the Pearson correlation coefficient of predicted value Y_1 and the 17 eigenvalues were calculated, as shown in Fig.2, and needed features were selected according to their absolute value.

3.1.2 Normalization

Firstly, the two features with smaller variance are eliminated and then the dimensionality of features is reduced to 8 (remaining $X_1, X_2, X_8, X_9, X_{12}, X_{14}, X_{15}, X_{16}$) from 15 by calculating and comparing the Pearson correlation coefficient. Dimensionality reduction has not only reduced the workload in an establishment of the prediction model but also can improve its performance. Then, the data is normalized by obtaining the average and standard deviation

of the remaining eight feature variables, therefore avoiding harmful effects may be caused by a wide difference between value ranges.

After the normalization of

$$\tilde{x} = \frac{x - \overline{x}}{S_X} \tag{3}$$

the average of variables will reach around 0, and standard deviation approaches 1. CART is used to make regression prediction of Y_1 ; the average error is 3.031, the error rate was 0.97%, the RMSE is 4.044. The red curve shown in Fig.3 is the actual value of Y_1 , and the green curve is the predictive value Y_1 .
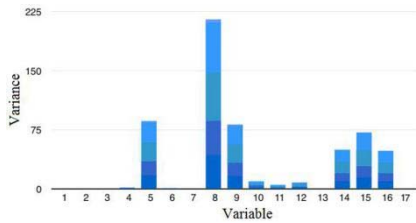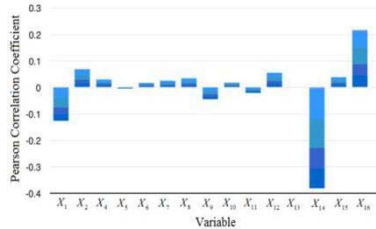

Fig.1. Feature Variance Histogram

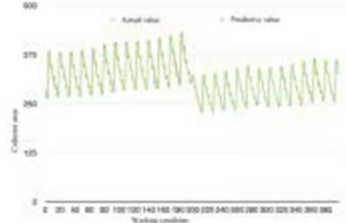Fig.2. Histogram of Each Feature Pearson Correlation Coefficient

Fig.3. Predictive Results of Collector Area Y_1

3.2 Performance Prediction on Y_2

Using 12 months as a period Y_2 , the multiple linear regression and least square method are adopted. The prediction expression of Y_2^1 for using the former 1600 groups of data as a training set and remaining 400 ones as a testing set is:

$$Y_2^1 = -15.972 + 0.002 X_1 + 0.001 X_2 + 0.359 X_3 + 0.009 X_4 + 0.002 X_7 - 0.005 X_8 + 0.003 X_9 + 0.001 X_{11} + 0.002 X_{12} \\ + 0.02 X_{15} - 0.253 X_{17}$$

The result is F=754.284, significance SIG=0.000. So it is judged at a probability of 99.9% that arguments $X_1, ..., X_{17}$ all have a significant effect on the dependent variable Y_2 and the RMSE is 0.006, quite ideal. Then each of results of 12 months can be obtained in turn, and the relationship between average monthly per meter borehole heat exchange of all 12 months and 17 inputs are formulated as $Y_2 = AX + b$

$$\text{where } Y_2 = \begin{bmatrix} Y_2^1 \\ Y_2^2 \\ \vdots \\ Y_2^{12} \end{bmatrix}, X = \begin{bmatrix} X_1 \\ X_2 \\ \vdots \\ X_{17} \end{bmatrix},$$

$$\beta = [-15.972, -10.942, -5.161, 6.281, 9.025, 8.461, 6.793, 7.060, 7.254, 4.010, -6.242, -14.701]$$

$$A = \begin{bmatrix}
0.002 & 0.001 & 0.359 & 0.009 & 4.476E{-}5 & 9.584E{-}5 & 0.002 & -0.005 & 0.003 & -2.697E{-}5 & 0.001 & 0.002 & -3.657E{-}6 & -7.087E{-}5 & 0.020 & 0.000 & -0.253 \\
0.002 & 0.000 & 0.302 & 0.006 & 3.668E{-}5 & 1.521E{-}5 & 0.001 & -0.004 & 0.001 & 1.906E{-}5 & 0.001 & 0.001 & -9.158E{-}5 & -2.411E{-}5 & 0.015 & 0.000 & -1.181 \\
0.001 & 0.001 & 0.175 & 0.003 & 3.269E{-}5 & -1.638E{-}5 & 0.001 & -0.002 & 0.000 & 3.462E{-}5 & 0.001 & 0.000 & 0.000 & 6.315E{-}6 & 0.007 & 0.000 & -0.079 \\
0.000 & 0.000 & 0.000 & -0.003 & 2.352E{-}5 & 0.000 & 0.001 & 0.002 & -0.001 & 0.000 & 0.001 & -0.001 & -0.001 & 0.000 & -0.010 & 0.000 & 0.105 \\
-0.002 & 0.000 & -0.249 & -0.005 & 8.010E{-}6 & -3.480E{-}5 & -0.001 & 0.003 & 0.000 & 0.000 & 0.000 & -0.001 & -0.001 & 0.000 & -0.024 & 3.041E{-}5 & 0.193 \\
-0.003 & -0.001 & -0.367 & -0.005 & 8.446E{-}6 & 0.000 & -0.003 & 0.003 & -0.001 & 0.000 & -0.002 & -0.001 & 0.000 & 0.000 & -0.027 & -3-399E{-}5 & 0.179 \\
-0.004 & -0.002 & -0.457 & -0.005 & 2.120E{-}5 & -0.001 & -0.006 & 0.003 & 0.000 & 0.000 & -0.003 & -0.001 & 0.000 & 0.000 & -0.017 & 0.000 & 0.123 \\
-0.003 & -0.001 & -0.360 & -0.005 & 2.947E{-}5 & -0.001 & -0.004 & 0.004 & 0.001 & 0.000 & -0.002 & -0.001 & 0.000 & 0.000 & -0.014 & 0.000 & 0.087 \\
0.000 & 2.873E{-}5 & -0.040 & -0.004 & 3.317E{-}5 & -3.088E{-}5 & 0.000 & 0.002 & -0.002 & 0.000 & 0.000 & -0.001 & 0.000 & 7.349E{-}5 & -0.001 & 0.000 & 0.079 \\
0.002 & 0.001 & 0.274 & -0.002 & 3.992E{-}5 & 0.000 & 0.002 & 0.002 & 9.690E{-}6 & -1.099E{-}5 & 0.002 & 1.671E{-}5 & 0.000 & -5.454E{-}6 & 0.014 & 0.000 & -0.018 \\
0.003 & 0.001 & 0.382 & 0.004 & 4.966E{-}5 & 0.000 & 0.003 & -0.002 & 0.000 & -7.226E{-}5 & 0.002 & 0.001 & 0.000 & -5.734E{-}5 & 0.021 & 6.179E{-}5 & -0.130 \\
0.003 & 0.001 & 0.384 & 0.008 & 4.850E{-}5 & 0.000 & 0.002 & -0.004 & 0.003 & -5.767E{-}5 & 0.001 & 0.002 & -2.506E{-}5 & -7.775E{-}5 & 0.022 & 0.000 & -0.265
\end{bmatrix}$$

3.3 Performance Prediction on Y_3

3.3.1 Seasonal factor decomposition

As can be seen from Section 2, Y_3 shows a cyclical downtrend. We can analyze this from the seasonal factor decomposition, and Fig.4 shows the seasonal factor decomposition results. The effect of seasonal factor item on time series is fixed and remains unchanged every year. The error term is a random value around 0. Due to that the appearance of error is random, we mainly explore the trend circulation item in time series. As we can see from Fig 4 (3), the trend circulation item shows a fluctuant downtrend.
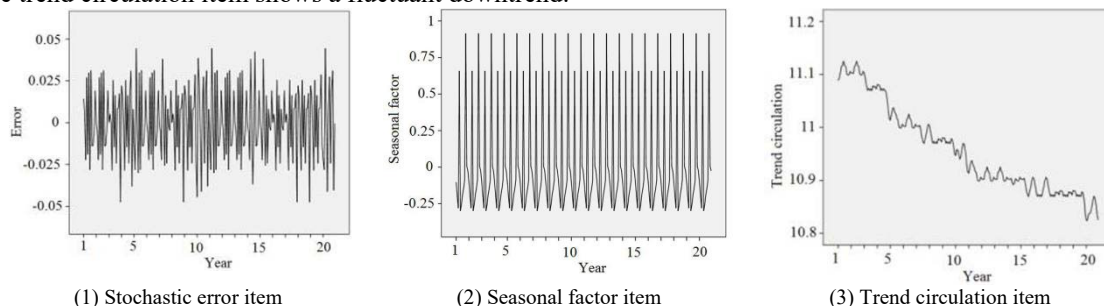

(1) Stochastic error item	(2) Seasonal factor item	(3) Trend circulation item

Fig. 4.Results of seasonal factor decomposition of Y_3

3.3.2 Time series analysis of Y_3

We use exponential smoothing method to predict the result after 20 years. The result respectively figured by (1) Simple non-seasonal model (Single exponential smoothing), (2) Simple seasonal model (Second exponential smoothing method) and (3) Holt-winters additive model (Triple exponential smoothing) show in Fig.5.

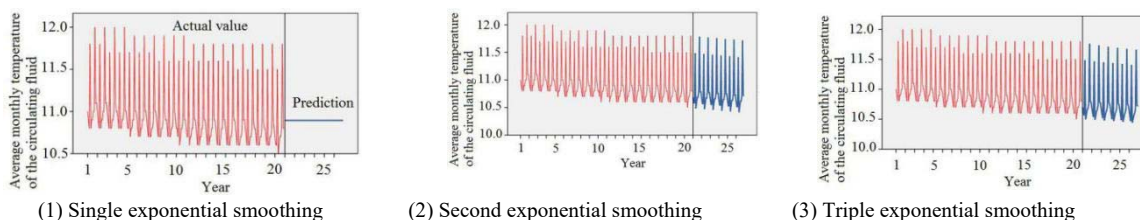| (1) Single exponential smoothing	(2) Second exponential smoothing	(3) Triple exponential smoothing

Fig.5. Predictive results of by Time series analysis

It can be seen that if we use a smoothing method, it is not able to predict the time series, and the predicted value is a straight line. Table 3 lists R^2, root-mean-square error (RMSE), Mean Absolute error percentage (MAPE), maximum absolute error percentage(MaxAPE), mean absolute error (MAE), maximum absolute error (MaxAE) and Standardized BIC.

Table 3. Various statistical indexes

	R2	RMSE	MAPE	MaxAPE	MAE	MaxAE	Standardized BIC
Second Exponential Smoothing Method	0.993	0.031	0.237	0.689	0.026	0.074	-6.973
Holt-winters Additive Model	0.994	0.030	0.226	0.634	0.025	0.070	-6.973

Simple seasonal model (Second exponential smoothing method) predicts the time series successfully, and the value of R^2 is 0.993. Holt-winters additive model (Triple exponential smoothing) also predict the time series successfully, and we can see the value of R^2 is 0.994. As is evident from the above methods, the Holt-winters additive model gets the maximum R^2 and the best prediction.

3.4 Performance Prediction on Y4

3.4.1 Seasonal factor decomposition

As can be seen from Section 2, Y_4 basically changes circularly and periodically, and the specific trend can be judged by seasonal decomposition.

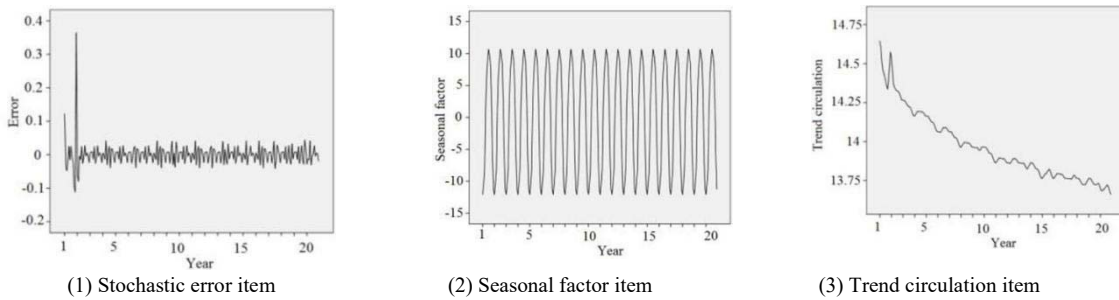| (1) Stochastic error item | (2) Seasonal factor item | (3) Trend circulation item |

Fig. 6. Results of seasonal factor decomposition of Y_4

From Fig.6, after seasonal decomposition, the effect of Seasonal factor item on time series is fixed and remains unchanged every year. The error term is a random value around 0. Fig.6 (3) shows that the trend circulation item also displays a fluctuant declining trend.

3.4.2 Time Series Analysis of Y_4

The prediction of Y_4 is performed by the Winters additive model in exponential smoothing method, and its result is shown in Fig.7.
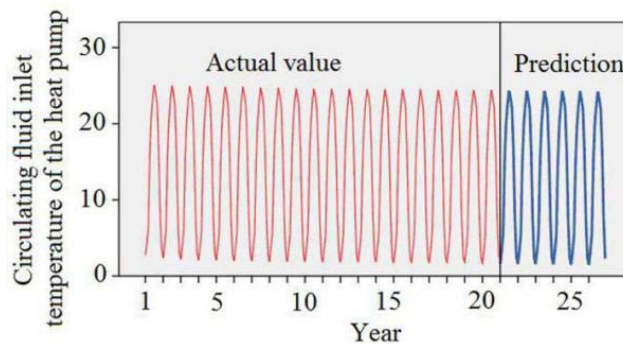

Fig. 7 Predictive results of by Time series analysis

Table 4. Various statistical indexes

	R2	RMSE	MAPE	MaxAPE	MAE	MaxAE	Standardized BIC
Holt-winters Additive Model	1	0.055	0.497	15.729	0.033	0.582	-5.740

It can be seen from Fig.7 that this Winters additive model has successfully predicted the time series Y_4, the Table 4 provides all the same statistical indexes as Table 3, and the value of R2 is 1, quite ideal.

3.5 Performance Prediction on Y_5

3.5.1 Seasonal Factor Decomposition

The results of seasonal factor decomposition for Y_5 are shown in Fig. 8. The results are similar with that of Y_4.
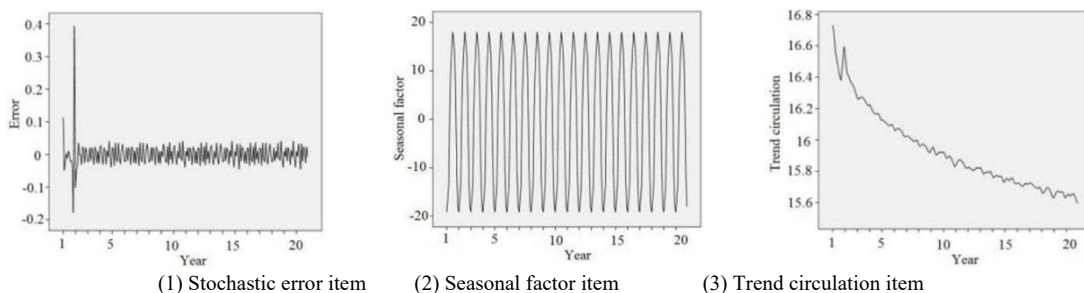
(1) Stochastic error item   (2) Seasonal factor item   (3) Trend circulation item

Fig. 8.Results of Seasonal Factor Decomposition of Y_5

3.5.2 Time Series Analysis of Y_5

The prediction of Y_5 is performed by the Winters additive model in exponential smoothing method, and its result is shown in Fig.9, and all statistical indexes of the prediction are listed in Table 5.
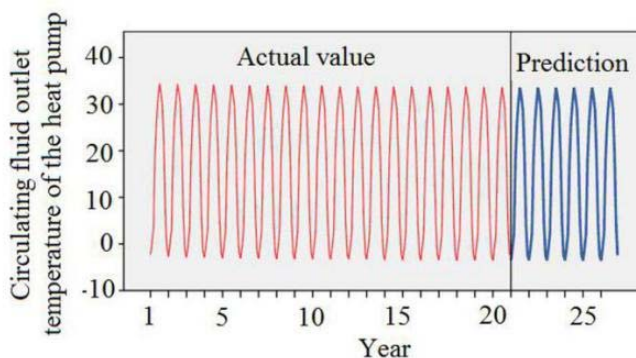

Fig. 9 Predictive results of by Time series analysis

Table 5. Various statistical indexes

	R^2	RMSE	MAPE	MaxAPE	MAE	MaxAE	Standardized BIC
Holt-winters Additive Model	1	0.055	1.442	59.417	0.032	0.594	-5.745

4. Conclusion

In this paper, we have shown that the collector area has been triumphantly predicted by Feature Selection based on variance and Pearson correlation coefficient together with CART with the average error of 3.031, the error rate of 0.97% and the RMSE of 4.044.The average monthly per meter borehole heat exchange has been predicted by multi-linear regression, and the relationship between average monthly per meter borehole heat exchange of all 12 months and 17 inputs are formulated as a matrix product form. The average monthly temperature of the circulating fluid, circulating fluid inlet temperature of the heat pump, circulating fluid outlet temperature of the heat pump has been successfully analyzed by seasonal factor decomposition, and their performances have been estimated by exponential smoothing. Experimental results demonstrate that the CART, multi-linear regression, seasonal factor decomposition and exponential smoothing are promising for practical applications in predicting performances of the solar-assisted GCHP systems.

Acknowledgements

Reference

[1] Tian Y, Wu W, Shi W, et al. An overview of the problems and solutions of soil thermal imbalance of ground-coupled heat pumps in cold regions. Applied Energy, 2016, 177:515-536.

[2] Yang W, Chen Y, Shi M, et al. Numerical investigation on the underground thermal imbalance of ground-coupled heat pump operated in cooling-dominated district. Applied Thermal Engineering, 2013. 58(1): 626-637.

[3] Chen X. and Yang H. Performance analysis of a proposed solar assisted ground coupled heat pump system. Applied Energy, 2012, 97:888-896.

[4] Verma V, Murugesan K. Experimental study of solar energy storage and space heating using solar assisted ground source heat pump system for Indian climatic conditions. Energy and Buildings, 2017. DOI: 10.1016/j.enbuild.2017.01.041

[5] Man Y, Yang H, Wang J. Study on hybrid ground-coupled heat pump system for air-conditioning in hot-weather areas like Hong Kong. Applied Energy, 2010, 87(9): 2826-2833.

[6] Man Y, Yang H, Spitler JD, Fang Z. Feasibility study on novel hybrid ground coupled heat pump system with nocturnal cooling radiator for cooling load dominated buildings. Applied Energy, 2011, 88(11): 4160-4171.

[7] You T, Wang B, Wu W, Shi W, Li X. Performance analysis of hybrid ground-coupled heat pump system with multi-functions. Energy Conversion and Management ,2015, 92:47-59.

[8] You T, Wang B, Wu W, Shi W, Li X. A new solution for underground thermal imbalance of ground-coupled heat pump systems in cold regions: Heat compensation unit with thermosyphon. Applied Thermal Engineering, 2014, 64(1): 283-292.

[9] Zhuang Z., Ben X, Yan R, et al. Accurately predicting heat transfer performance of ground heat exchanger for ground-coupled heat pump systems using data mining methods. Neural Computing and Applications, 2016. DOI: 10.1007/s00521-016-2307-7

[10] Cui P, Man Y, Fang Z. Geothermal Heat Pumps. Renewable Energy, DOI: 10.1002/9781118991978.hces041